Eur Radiol (2002) 12:2352–2364
DOI 10.1007/s00330-001-1256-3



**J.D. Spratt**
**A.J. Stanley**
**A.J. Grainger**
**I.G. Hide**
**R.S.D. Campbell**

# The role of diagnostic radiology in compressive and entrapment neuropathies

Received: 30 July 2001
Revised: 9 November 2001
Accepted: 16 November 2001
Published online: 19 April 2002


J.D. Spratt · A.J. Stanley · I.G. Hide
R.S.D. Campbell (✉)
Department of Radiology,
James Cook University Hospital,
Middlesbrough, TS4 3BW, UK
e-mail: Rob.Campbell@stees.nhs.uk
Tel.: +44-1642-850850 ext. 3975
Fax: +44-1642-854611

A.J. Grainger
Department of Radiology,
Leeds General Infirmary, Leeds, UK

**Abstract** Diagnostic imaging is increasingly being utilised to aid the diagnosis of compression and entrapment neuropathies. Cross-sectional imaging, primarily ultrasound and magnetic resonance imaging, can provide exquisite anatomical detail of peripheral nerves and the changes that may occur as a result of compression. Imaging can provide a useful diagnostic aid to clinicians, which may supplement clinical evaluation, and may eventually provide an alternative to other diagnostic techniques such as nerve conduction studies. This article describes the abnormalities that may be demonstrated by current imaging techniques, and critically analyses the impact of imaging in diagnosis of peripheral compressive neuropathy.

**Keywords** Neuropathy · MRI · Ultrasound

## Introduction

Compressive and entrapment neuropathies (CEN) are relatively common, especially in patients with predisposing occupations or with certain medical disorders. They are caused by mechanical or dynamic compression of a short segment of a single nerve at a specific site, frequently as it passes through a fibro-osseous tunnel or an opening in fibrous or muscular tissue. Any or all layers of the nerve, including the endo/epi/perineurium, intraneural microvessels or Schwann cells may be injured, accounting for the variability of pathological features, which vary from a transient conduction block through total demyelination to neural fibrosis and Wallerian degeneration. Identification of the level of nerve injury depends on knowledge of the anatomic course and innervation pattern applied to a carefully taken clinical history and thorough neurological examination including various provocative tests and in selected cases on electromyography, motor and sensory nerve conduction and velocity studies [1].

Electrodiagnosis yields a significant false-negative rate in CEN (up to 30%) perhaps due to anomalous innervation and only partial damage to fast-conducting fibres [2]. The technique suffers from a lack of precise anatomical localisation in areas where numerous small muscles are present. Several specialized techniques may be utilised to increase the diagnostic yield in CEN [3]. Over-diagnosis is recognized when age and anthropometric measures are not considered [4]. The detection of fibrillation potentials in electromyography is helpful in the diagnosis of severe CEN where axonotmesis has occurred, but the discomfort of multiple needle insertions may make it impossible to perform, especially in children, and complications may increase in patients with immunocompromise and bleeding diatheses [2]. Accurate placement of needles into deeper smaller muscles, e.g. pronator quadratus, may also be difficult. In all instances, the value of electrodiagnosis is only as good as the skill of the clinical electrophysiologist performing the studies and the clinician in correlating this information with the clinical examination, who may be unaware

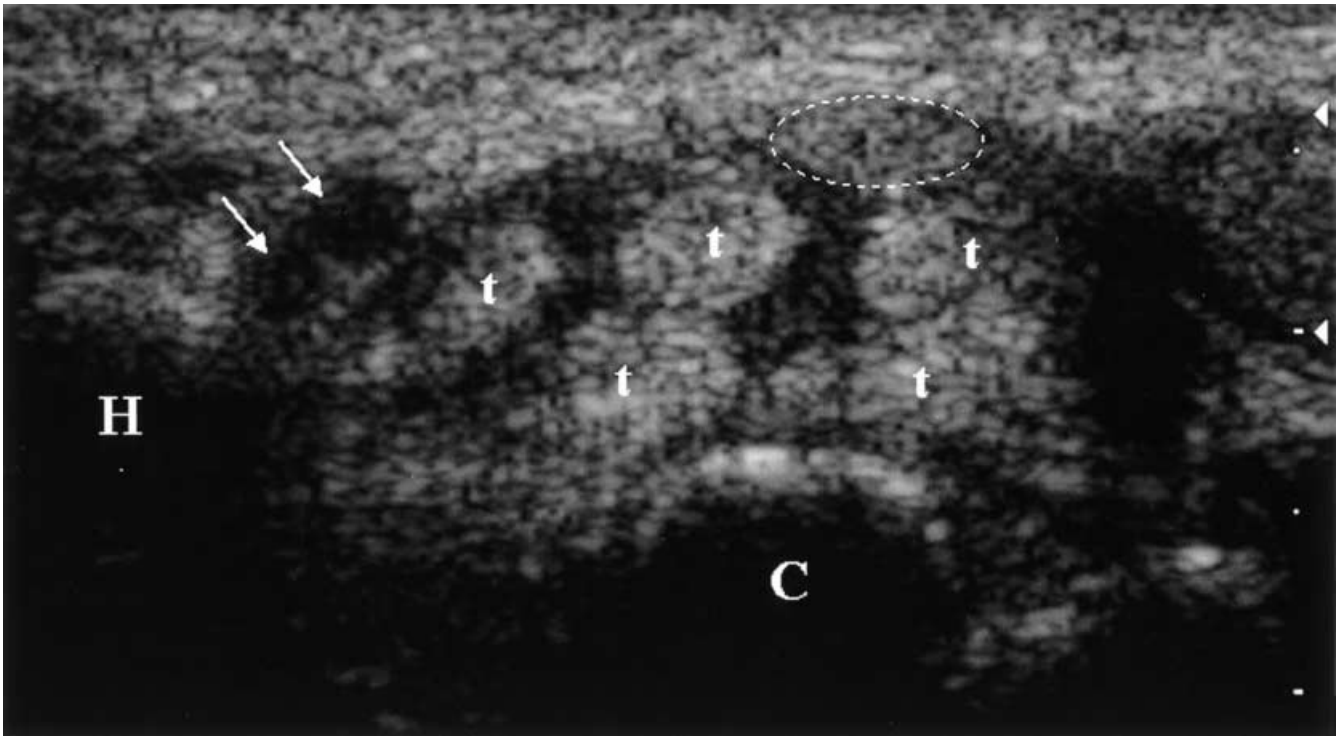


**Fig. 1** Transverse US image of the wrist in a patient with carpal tunnel syndrome (CTS). The image is taken at the level of the hamate (*H*) and capitate (*C*). The median nerve (*dotted oval*) is thickened (cross-sectional area=13 $mm^2$), and there is low reflective change around the flexor tendons (*t*), indicating the presence of tenosynovitis. Bowing of the flexor retinaculum is evident. The ulnar vessels within Guyon's canal are also demonstrated (*arrows*)

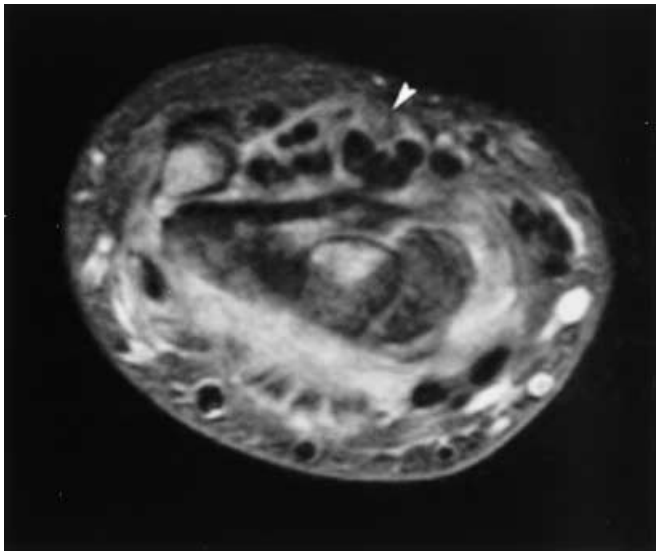

**Fig. 2** Axial short tau inversion recovery (STIR) image of the wrist in a patient with sarcoidosis. Clinical features of both ulnar and median nerve entrapment were present. There is extensive high signal present around the wrist joint, resulting from synovitis and tenosynovitis. The median nerve (*arrowhead*) is thickened but does not demonstrate increased signal intensity

of the problems and pitfalls in performing and interpreting these tests.

This article critically analyses the role of radiology in three areas relevant to CEN, namely imaging the (a) compressive lesion, (b) affected nerve and (c) affected muscles.

## Imaging of the compressive lesion

Imaging may be used to help diagnose the presence of an extrinsic compressive lesion and assist in surgical planning. Plain X-ray techniques have a limited use in CEN evaluation due to poor soft tissue contrast resolution. However, bony abnormalities can lead to CEN. Osteophytes of the medial humeral epicondyle can entrap the ulnar nerve, and carpal dislocation may compress the median nerve [5]. Osteochondromata may be encountered at any site in the skeleton, and malaligned fractures (e.g. of the proximal fibula affecting the common peroneal nerve) or callus (e.g. from clavicular fractures affecting the lower trunk of the brachial plexus) may result in neural compression. Calcified/ossified soft tissue lesions, such as gouty tophi or haemangiomas, may be visualised. The space-occupying effects of soft tissue masses causing splaying of adjacent bones or bony erosion may also be encountered.

The high spatial resolution and exquisite flow detection methods of US allows analysis of many superficial soft tissue structures. Abnormalities, such as tenosynovitis, synovial hypertrophy, ganglia, giant cell tumour of the ten-

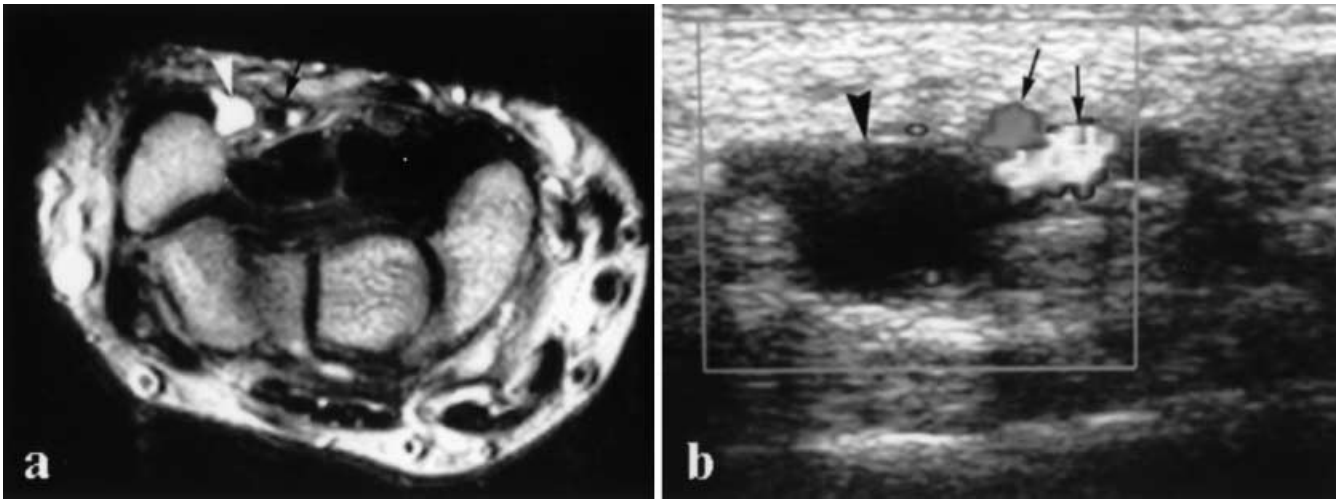


**Fig. 3** Axial T2-weighted MR image of the wrist at the level of **a** the pisiform, and **b** the corresponding transverse colour Doppler US demonstrate a ganglion within Guyon's canal (*arrowheads*). The ganglion has typical high signal on the T2-weighted image, with low reflectivity on US. The ulnar nerve lies between the cyst and the adjacent ulnar vessels, which are clearly demonstrated both on MRI and colour Doppler imaging (*arrows*)

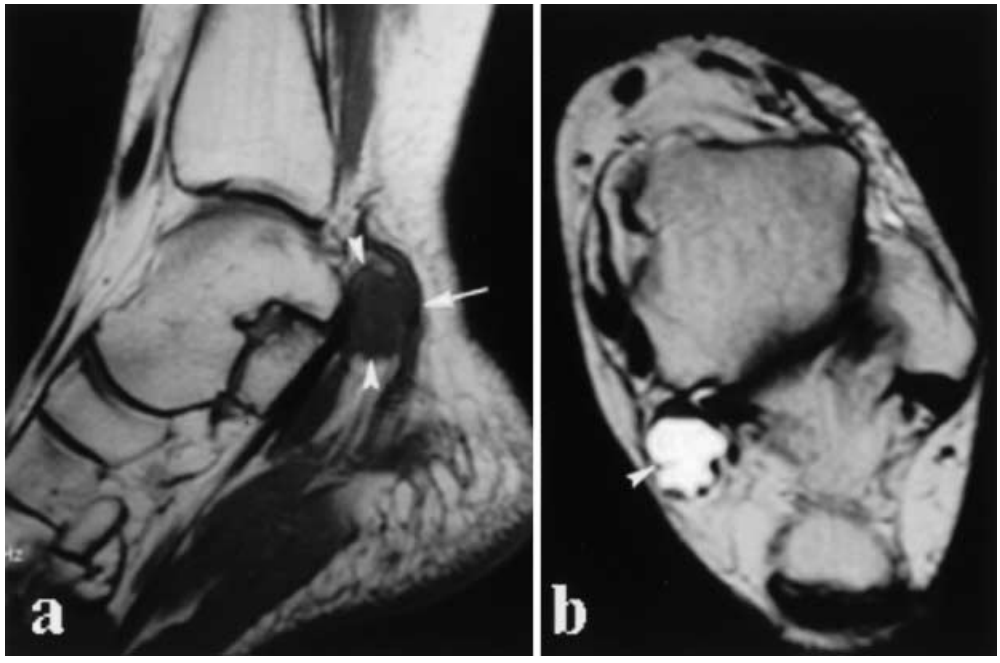


**Fig. 4** **a** Sagittal T1-weighted MR image and **b** axial T2-weighted image of the ankle in a patient with medial foot pain. There is a ganglion cyst (*arrowhead*) arising from the flexor hallucis longus tendon causing compression of the posterior tibial nerve in the tarsal tunnel. The tibial vein lies posterior to the cyst (*arrow*), which has the characteristic signal intensity of fluid, with intermediate signal intensity on the T1-weighted image and high signal on the T2-weighted image

don sheath (GCTTS), lipomas, aberrant musculovascular anatomy and bursae, metabolic oedema and infiltrative processes (e.g. amyloidosis), have all been identified as causes of carpal and tarsal tunnel syndromes (Figs. 1, 2) [6, 7, 8]. Carpal tunnel syndrome caused by tophaceous gout has also been described on CT and MRI [9].

Vascular pathology, such as pseudoaneurysm or thrombosis of the ulnar artery in Guyon's canal, may compress the ulnar nerve, or the nerve may be trapped between a mass and the ulnar artery (Fig. 3). Spinoglenoid notch arteriovenous malformation (AVM) causing compression the suprascapular nerve has also been described [10].

Ganglion cysts are common and usually possess characteristic ultrasonic features, with a well-defined border enclosing homogeneously hyporeflective cystic contents. Such cysts often originate from a tendon sheath (Fig. 4), but intra-neural cysts, which invest the neural sheath may also be encountered (Fig. 5). Therapeutic US-guided aspiration and steroid injection of ganglia causing CEN in the hand has been reported [11, 12]. Paralabral cysts and ganglia are another cause of entrapment of the suprascapular

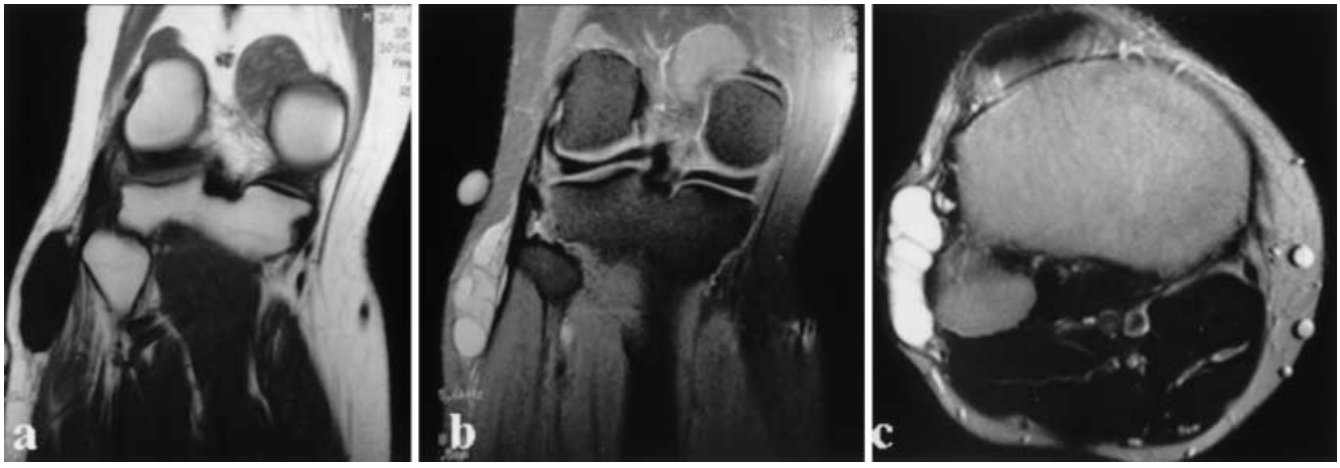


**Fig. 5** Intraneural ganglion of the peroneal nerve confirmed at surgery. The patient presented with foot drop, which partly recovered. The mass has typical signal characteristics of a loculated cyst on **a** the coronal T1-weighted, **b** the coronal short tau inversion recovery (STIR) and **c** axial T2-weighted images. The peroneal nerve cannot be identified separate from the cyst on the MR images, and intraneural involvement can only be postulated at imaging

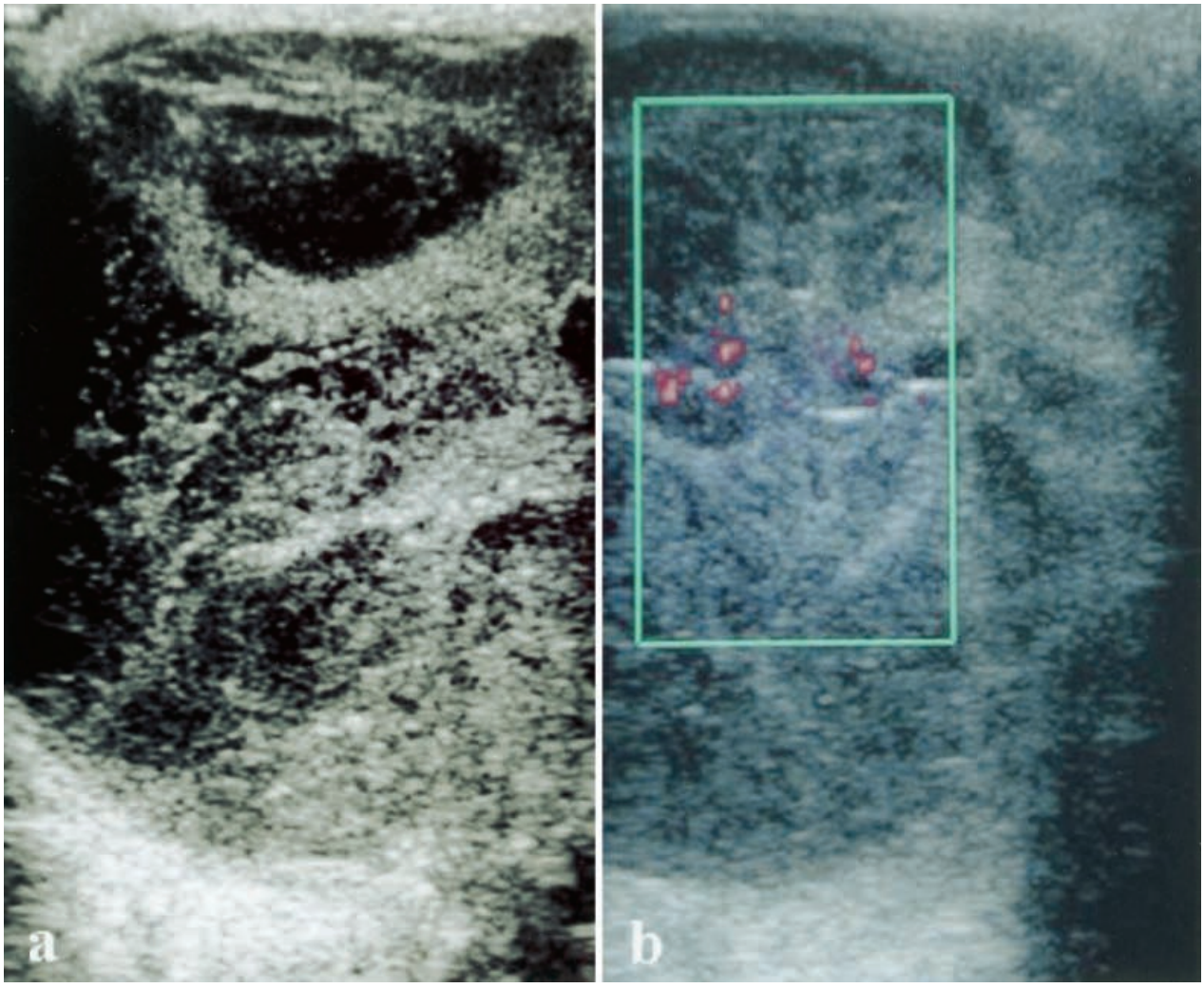


**Fig. 6a, b** Giant cell tumour of the tendon sheath in a patient with tarsal tunnel syndrome. **a** The grey-scale image demonstrates a large mass with heterogeneous reflectivity, acoustic enhancement, and vascularity on **b** colour Doppler imaging. The flexor tendons were inseparable from the mass, and the posterior tibial nerve could not be identified

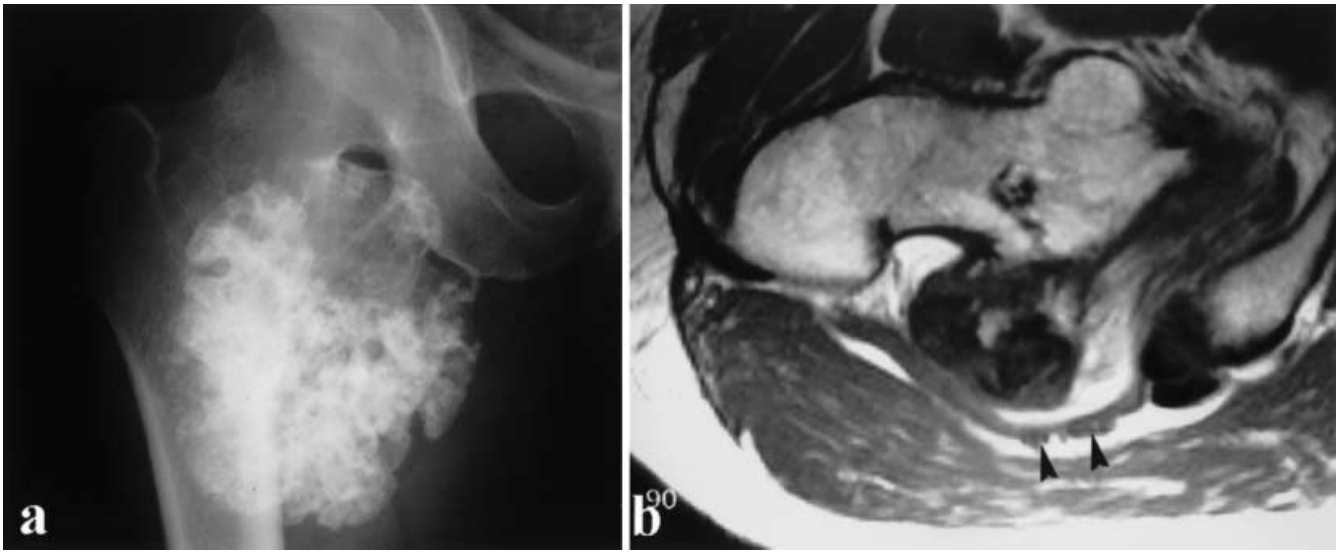


**Fig. 7a, b** Images from a patient who presented with symptoms of sciatic nerve compression. **a** Plain radiographs show a large osteochondroma, which was subsequently demonstrated to have chondrosarcomatous degeneration. **b** The axial T1-weighted MR image shows part of the osteochondroma with the sciatic nerve and one of its divisions stretched over the mass posteriorly (*arrowheads*)

nerve, and again US-guided drainage may be performed [13]. Synovial cyst formation should be considered as a possible cause of CEN in patients with post-traumatic, degenerative and inflammatory processes occurring in and around joints, for example, cubital tunnel at the elbow [14] or even post arthroplasty at the knee [15]. The GCTTS, unlike typical ganglion cysts, have internal echoes, lack posterior acoustic enhancement and can show internal vascular signals on colour Doppler US (Fig. 6) [16].

Sonography of the cubital tunnel may reveal prominent osteophytes from the medial epicondyle of the humerus, a thickened retinaculum or anomalous muscle (anconeus epitrochlearis), which may result in static compression, scar fixation or traction of the ulnar nerve [17]. An accessory flexor muscle in the carpal tunnel may also be a cause CEN. Ultrasound reveals a hyporeflective mass adjacent to tendons with the typical striated appearance of muscle, and dynamic evaluation reveals the changes in the shape of the muscle mass. Although MRI may also be helpful in evaluating the size and location of anomalous muscle, the signal intensity can be similar to lesions such as GCTTS [18], and MRI lacks the dynamic nature of US which allows easy identification of normally contracting muscle.

Both MRI and US may be used to detect superficial soft tissue lesions, but MRI is the primary modality for investigation of deeper soft tissue structures and where associated bone abnormalities are present. Acute sciatic and superior and inferior gluteal nerve compression has been described with chondrosarcomatous degeneration in hereditary multiple exostoses (Fig. 7) [19]. Magnetic resonance imaging is also the method of choice for evaluating patients with non-traumatic brachial plexopathy: radiation fibrosis, primary and metastatic lung cancer and breast cancer account for almost three-quarters of the causes [20, 21]. Magnetic resonance imaging can diagnose benign aggressive processes affecting the lumbosacral plexi such as desmoid tumour or endometriosis. Magnetic resonance imaging has also proved useful in differentiating recurrent tumours infiltrating nerves from scarring or compressive neuropathy due to regional deformity where clinical examination and routine investigations were unhelpful [22]. Magnetic resonance imaging can differentiate cervical rib and scalene anticus syndromes from viral brachial plexitis (Parsonnage-Turner syndrome) [23]. Functional imaging of thoracic outlet syndrome has been utilised, in open MR systems, as a diagnostic tool to diagnose brachial plexus compression on coronal reformatted images with the arm in varying degrees of abduction [24]. Posterior interosseous nerve compression from an enlarged bicipital bursa has been confirmed by MRI [25]. Synovial chondromatosis affecting the annular peri-radial recess of the elbow joint causing posterior interosseous nerve palsy has also recently been documented on MRI, although the described features were non-specific [26]. Magnetic resonance imaging may also provide information regarding pathology associated with compressive lesions which is not apparent sonographically, e.g. glenoid labral tears associated with paralabral cysts of the spinoglenoid notch [27].

## Imaging of the affected nerve

Numerous papers have assessed the ability of US and MR imaging to document secondary intraneural changes in CEN, particularly the median nerve in carpal tunnel

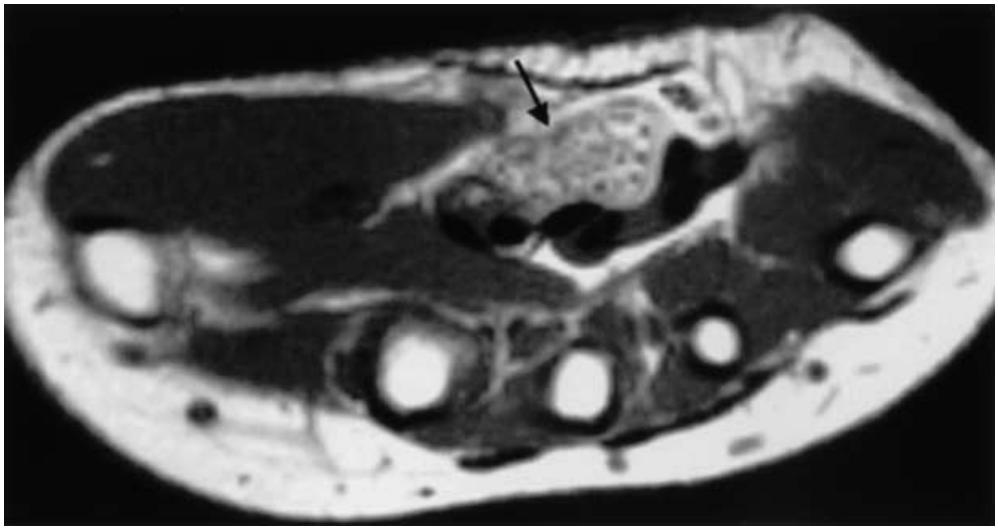

**Fig. 8** Axial T1-weighted MR image of a fibro-lipomatous hamartoma of the median nerve. High signal intensity fat is seen dispersed around the divisions of the median nerve (*arrow*), within and distal to the carpal tunnel

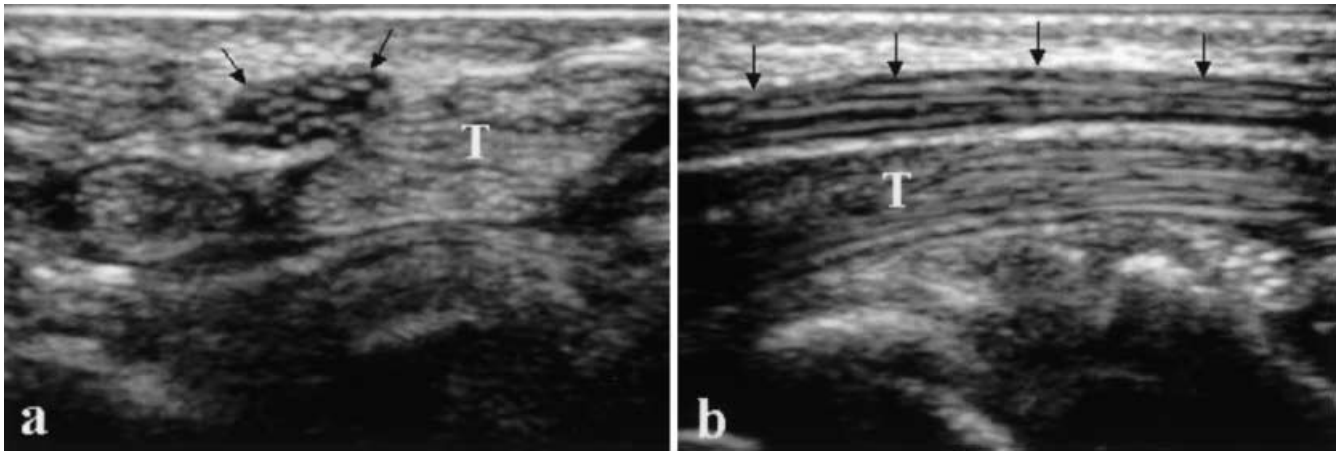


**Fig. 9** High-resolution **a** transverse and **b** longitudinal US images of a normal median nerve (probe frequency 7–15 MHz). The median nerve (*arrows*) is seen as a well-defined fibrillar structure with low reflective longitudinal bundles interspersed with reflective interfascicular epineurium, which appear as bright dots on the transverse image. The flexor tendons (*T*), which lie deep to the nerve, exhibit higher reflectivity

syndrome. Imaging is also able detect primary intrinsic lesions of the nerve, such as schwannoma, neurofibroma and fibrolipomatous hamartoma (Fig. 8). These lesions may present with symptoms similar to extrinsic compression and classically demonstrate ultrasonic continuity with the nerve of origin [28]. Nerve compression in osteofibrous tunnels has been described in leprosy with enlarged nerves exhibiting both abnormal and absent fasicular morphology [29].

## Normal US appearance

High-frequency US equipment (7–12 MHz) is able to identify nearly all the main nerve trunks running in the limbs and extremities. The commonest sites of CEN that are amenable to direct ultrasonic nerve visualisation include the carpal tunnel for the median nerve, the cubital tunnel and Guyon's canal for the ulnar nerve, the proximal fibula for the common peroneal nerve and the metatarsal heads for the interdigital nerves of the foot [2, 7, 30, 31, 32, 33]. Unfortunately, some smaller nerves that can be affected by CEN, such as the anterior interosseous nerve, may not be directly visualized [34, 35].

Nerves can be differentiated from adjacent tendons using specific anatomical landmarks, different behaviour during dynamic study and their fascicular vs fibrillar echotexture [28]. Close observation reveals the echotexture of normal nerves to be composed of discrete discontinuous longitudinal bands (fascicles) of low reflectivity interposed by high reflectivity stripes (interfascicular epineurium) and on transverse section the low reflectivity bands become rounded embedded in a hyper-reflective background (Fig. 9) [36]. If the probe is not perpendicular to the nerve, it appears hyporeflective, due to anisotropic effects, which may be confused with intraneural pathology.

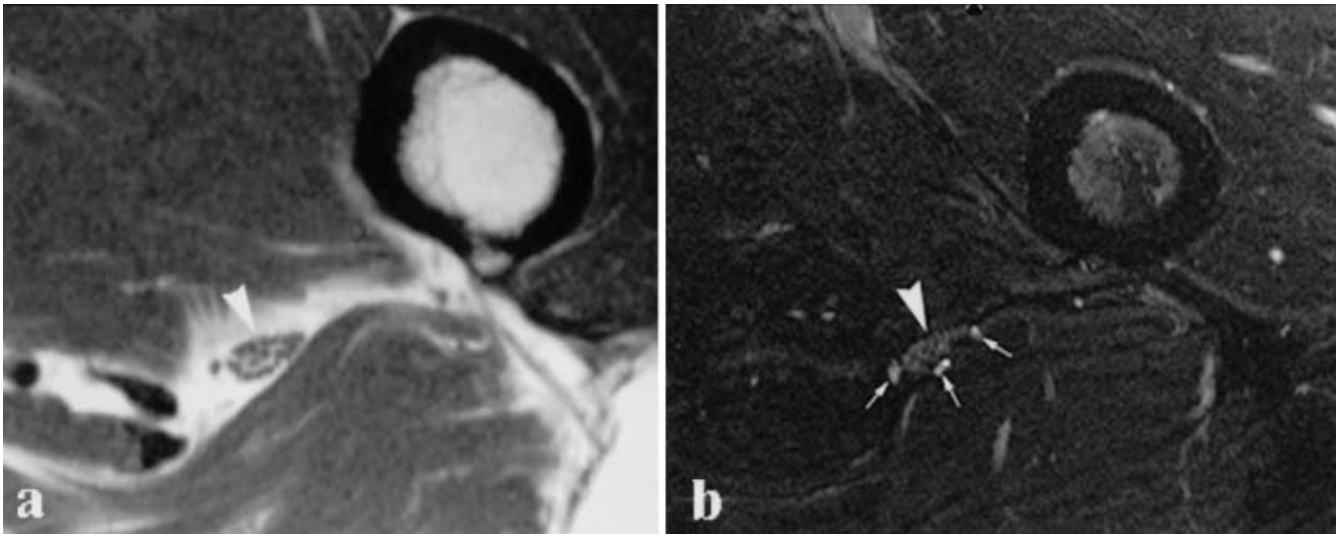


**Fig. 10** **a** Axial T1-weighted image and **b** STIR image of a normal sciatic nerve (*arrowhead*), just distal to the level of the lesser trochanter. The fascicular nature of the nerve is appreciated on the T1-weighted image, whereas on the STIR image subtle increased signal within the nerve represents endoneural fluid. Three tiny vessels adjacent to the nerve can also be visualised on the STIR image (*arrows*)

## Normal MRI appearance

Many nerves are well visualised by MRI using T1-weighted images to display regional anatomy and fat-suppression techniques to detect pathological signal change within a nerve. Fat signal around the nerve and within the interfascicular epineurium is suppressed. Short tau inversion recovery (STIR) sequences provide the most uniform and consistent fat suppression while maintaining excellent T2 contrast. (Frequency-selective fat saturation sequences may result in poorer nerve visualisation due to "bleed-through" of fat signal in some areas and suppression of the water signal in others.) Image quality can also be improved by the use of flow saturation bands, which greatly attenuate phase-shift artefacts from blood flow [37, 38, 39]. Magnetic resonance images are obtained in at least two planes guided by the clinical and neurological findings. The long-axis images of the nerve help detect displacement or focal enlargement and axial images allow detection of T2 signal changes by reducing partial-volume effects. Spatial relationships to other tissues are not always helpful because nerves change both shape and location with changes in joint position [22, 40, 41]. Positive nerve identification must rely on internal appearance and analysis of multiple contiguous images, rather than the relations to non-neural tissues on a single image alone. Visualisation of the characteristic clustered dot-like appearance of the fascicles on axial T2-weighted images is assumed to be due to the signal from endoneural fluid (Fig. 10) [37, 39, 41].

## US appearances of neural compression

In cases of CEN, US may detect neural flattening at the site of compression with nerve swelling proximally. There may also be loss of the normal fascicular pattern and gain of uniform low reflectivity, possibly due to intraneural venous congestion and oedema in the interfascicular epineurium and perineural plexus [28], similar to that reported on dynamic MRI [42, 43]. These changes may be subtle and comparison with the opposite side may be helpful.

Quantitative analysis has been performed for the median nerve at the carpal tunnel: The "swelling ratio" – the ratio of the mean cross-sectional area of the nerve at the levels of the pisiform and distal radioulnar joint – is abnormal over 1.3, and the "flattening ratio" of the nerve's major to minor axis at the level of the hamate is abnormal over 3.4 [31, 44]. Although initial reports had suggested that the "flattening ratio" of the median nerve had a poor predictive value [45], the recent study by Keberle et al. utilised angle-corrected measurements for diagnosis of carpal tunnel syndrome (CTS) [44]. The real-time dynamic application of US may be seen in the reduced transverse sliding of the median nerve under the flexor retinaculum in CTS, which may be helpful when nerve measurements are borderline or indeterminate [43]. Ultrasound may also detect variants such as proximal bifurcation or accessory branches of the median nerve. This is important to recognise prior to endoscopic release to avoid inadvertent resection of these aberrant bundles [6]. Morton's neuroma, thought to be caused by repetitive trauma of the plantar interdigital nerves beneath the intermetatarsal ligaments leading to hypertrophy of intraneural connective tissue and hyalinisation of endoneural vessel walls, may appear as well-defined or ill-defined, ovoid masses of low reflectivity elongated along the axis of the metatarsals [46]. Ultrasound has demonstrated sensitivity and specificity as high as 100 and 83% respectively, in the diagnosis of Morton's neu-

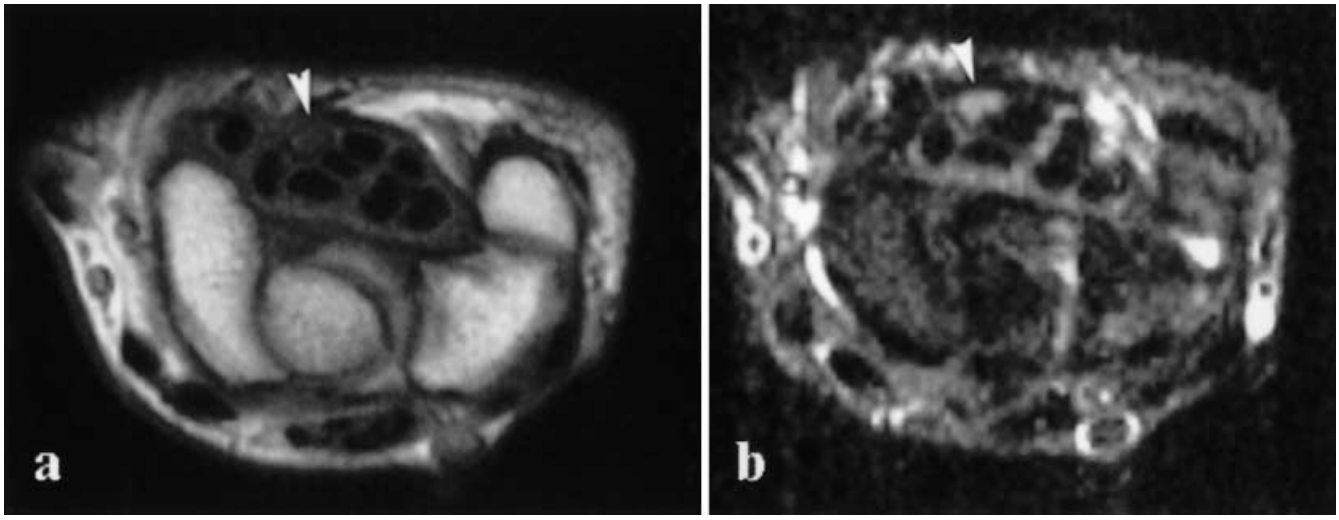


**Fig. 11** **a** Axial T1-weighted image and **b** STIR image of the wrist. High signal is evident within the median nerve on the STIR sequence (*arrowhead*); however, this finding is not considered to be highly specific for neural compression, and may be reproduced with strong contrast windowing. This patient had no symptoms of CTS

roma, and can guide surgery to the appropriate intermetatarsal space [47, 48].

## MRI appearances of neural compression

Focal loss of the perineural fat plane is demonstrated on T1-weighted MR images in association with compressive lesions; however, this appearance may be normal in younger, thinner patients. A focal abnormal fascicular pattern may be seen, either as a total absence of visualized fascicles or as heterogeneity in fascicular size. The presence of focal abnormal T2 signal, perhaps representing increased fluid in the endoneural spaces, is thought by some to be the most reliable finding to confirm the diagnosis of CEN, to eliminate the possibility of a mass lesion and to help with surgical planning and post-surgical follow-up [49]. However, the assessment of increased signal is subjective, may be affected by variations in window levels and has been shown to be less useful than other MR signs of CEN (see discussion below; Fig. 11).

As with US, MRI has also been shown to be of potential value in the diagnosis of CTS [50, 51, 52, 53, 54, 55, 56, 57, 58, 59, 60]. However, the predictive value of many of the reported MR features of CTS has been the subject of speculation and controversy. A recent large consecutive series recruiting a wide spectrum of patients with a low incidence of CTS [56] revealed many of the MRI signs to have poorer specificities than originally stated in several smaller series which used volunteers as controls [57, 58, 59, 60]. The low sensitivities of all previously described signs were confirmed. In this study, retinacular bowing, median nerve flattening and deep palmar bursitis all had specificities greater than 94%, whereas proximally increased nerve size, increased nerve signal, flexor tenosynovitis and decreased deep tendon fat had poorer specificities. Another recent small series using a 3-T magnet with study design similar to that of the initial reports confirms retinacular bowing as a strong predictor of CTS, but suggests that a 50% size increase of the nerve both proximal to, and within, the carpal tunnel is significant (Fig. 2) [61].

It has been suggested that it is necessary to measure cross-sectional area (CSA) of the median nerve, as subjective assessment alone has proven insufficiently diagnostic [57, 62, 63, 64]. However, the cut-off point between normality and pathological enlargement is unclear. A mean CSA of the normal nerve of 10–11 $mm^2$ has recently been reported on MRI [61] compared with previous MRI reports of 6–9 $mm^2$ [59, 63, 65] using similar T1- and T2-weighted sequences. These differences are unexplained.

Some authors believe MRI may be better than sonography in subtle cases of CTS because of its soft tissue contrast and its additional diagnostic feature of showing signal changes caused by oedema [31, 57, 59, 63, 64]. However, Keberle et al. directly compared MRI and US, yielding 100% sensitivity in CTS diagnosis with both modalities, using the angle correction method [44]. No papers have yet addressed the impact of MR imaging on patient management or outcome.

The MRI features of other CENs have been described, including the ulnar, median and radial nerves at the elbow [66], but again the clinical impact of imaging has not been proven.

## Future developments in nerve imaging

There have been reports of MRI protocols that dramatically increase the conspicuity of nerves using rapid ac-

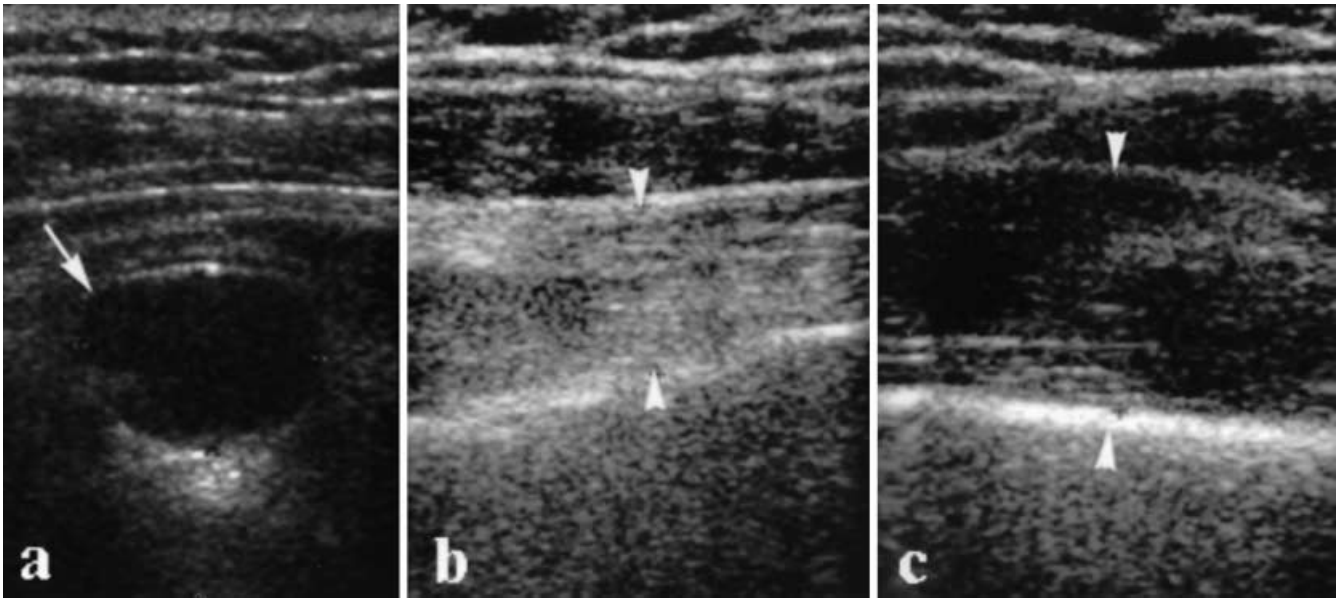


**Fig. 12a, b** Ultrasound images of a patient with isolated wasting of the infraspinatus muscle secondary to compression of the suprascapular nerve. **a** A large cyst with low reflectivity is present in the spino-glenoid notch (*arrow*). **b** The ipsilateral infraspinatus muscle is reduced in bulk with increased reflectivity (*arrowheads*), compared with **c** the normal contralateral side, representing fatty atrophy

quisition of imaging data and phased-array radiofrequency (RF) coil technology. Larger nerves can be so well demonstrated with these techniques that maximum intensity projection (MIP) post-processing software can be utilised to create "MR neurograms" [37, 38, 39]. Integrated data from phased-array coils produces a higher signal-to-noise ratio with a larger combined field of view [67]. In locations such as the carpal tunnel, the precise location by MR neurography may help to distinguish proximal from distal compression and thus allow for smaller exposures or percutaneous approaches without increasing the risk of failure due to inadequate release in non-standard cases [37]. Neuromuscular variants, such as those described passing through the femoral nerve within the pelvis, may have potential for CEN [68], and MR neurography might provide means for imaging such proximal, relatively larger obliquely intersecting structures, perhaps as a guide to laparoscopic release; however, the accuracy, sensitivity and clinical utility of this new technique remain to be established.

Advances in peripheral nerve imaging by MRI depends on further improvements in RF coil technology and pulse sequence design that allow higher-quality images in a shorter time and perhaps the application of functional imaging techniques. Diffusion-weighted imaging, already shown to depict subtle abnormalities within the white matter tracts of the human brain due to reduction of diffusion anisotropy along the axons, has been shown to be a feasible diagnostic tool in animal peripheral nerves [69]; however, the smaller size of human nerves and the susceptibility artefacts noted above complicate their depiction and require gradient fields too strong for clinical applications [70]. Contrast agents presently do not offer a reliable alternative for current protocols for direct nerve imaging. Intravenous gadolinium enhances nerves in a variable fashion, differing from site to site along a single nerve whether or not the nerve is affected by pathology [49] and intraneural MR contrast agents (for delivery by axonal transport) remain at an early stage in their development [71]. Two-dimensional gradient-recalled-echo magnetisation transfer sequences were found to be more sensitive than T1-weighted spin echo in demonstrating perineural contrast enhancement in CTS, the latter feature being especially useful in the post-operative patient [72].

Improvements in US technology with higher-frequency probes, and techniques such as compound imaging which help reduce anisotropic effects, image noise, and other acoustic phenomena allow a more detailed analysis of superficial neural structures [73]. Recently, refined US measurement techniques have led to significantly improved comparative results in CTS diagnosis [44].

## Imaging of the affected muscle

In the frequently encountered situation where cross-sectional imaging cannot demonstrate abnormality of the affected nerve, or a compressive lesion as the cause of a neuropathy, imaging of regional muscles may identify abnormality in a characteristic group which are normally innervated by the nerve from a typical level, hence localizing the level of neural entrapment.

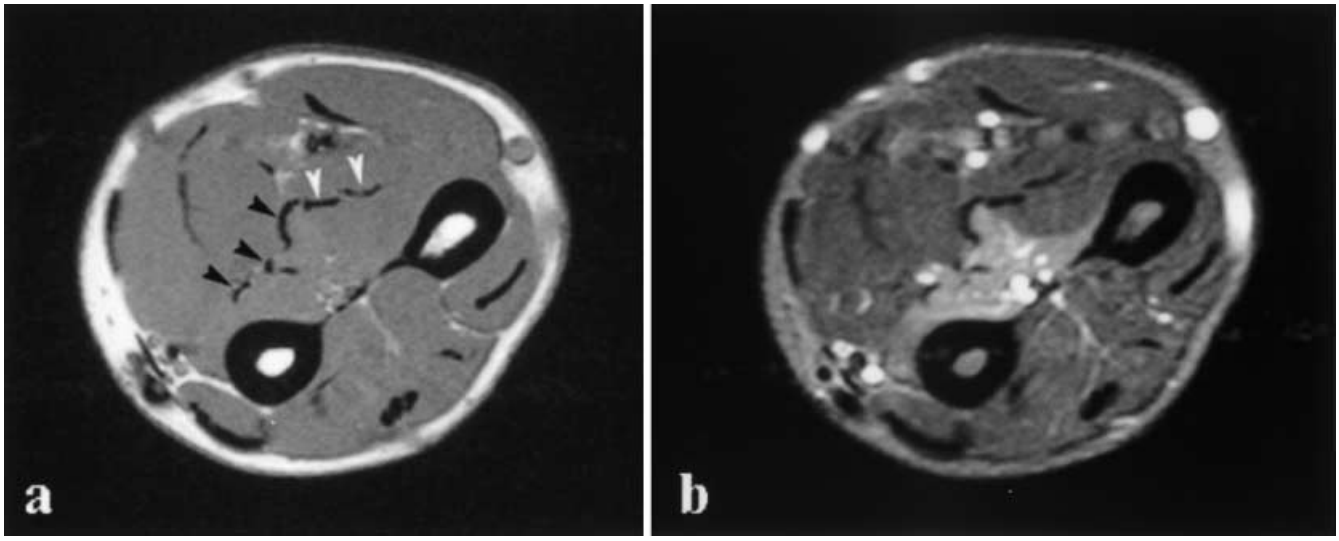


**Fig. 13** **a** Axial T1-weighted and **b** STIR images of the forearm in a patient with anterior interosseous nerve syndrome. The tendons to flexor pollicis longus, and the flexor digitorum profundus (FDP) to index and middle fingers (*black arrowheads*), is seen adjacent to their respective muscle bellies, which demonstrate loss of bulk and increased signal intensity on the STIR image, secondary to denervation. Conversely, the muscles adjacent to the tendons of the ring and little finger FDP (*white arrowheads*) are normal and do not demonstrate features of denervation. (From [77])

Ultrasound can demonstrate denervation changes in muscle, the earliest occurring at 10 days post injury [74], although its sensitivity and specificity remain unproven. Loss of muscle bulk and increased reflectivity may be apparent (Fig. 12). Reduced perfusion on Doppler sonography and relative lack of active contraction of the affected muscles have also been described [35].

Magnetic resonance imaging is useful in detecting and characterizing denervation atrophy and neurogenic oedema in shoulder muscles [10, 27, 75, 76]. Fatty atrophy of teres minor due to an axillary nerve cyst and quadrilateral space syndrome have been documented [76] as well as solitary atrophy of infraspinatus due to spinoglenoid notch arterio-venous malformation [75]. Paralabral cysts may entrap the suprascapular nerve either at the scapula notch (compressing both motor branches) or near the spinoglenoid notch (selectively involving the nerve to infraspinatus).

Short tau inversion recovery MR images demonstrate increased extracellular water in the subacute phase of denervation and T1-weighted images reveal homogeneous atrophy and fatty change in the irreversible chronic phase of muscle denervation [10]. The STIR MR imaging of forearm muscles may serve as a useful adjunct to electromyography in the investigation of anterior interosseous nerve syndrome (Fig. 13) [77]. Fat-saturated fast T2-weighted spin-echo sequences have also been used to demonstrate subacute denervation [76]. Magnetic resonance is unreliable in depicting acute denervation, the initial changes occurring by 2 weeks [10, 75]. It has been suggested that the degree of signal change on STIR MRI sequence correlates well with the degree of denervation seen on EMG and weakness found on clinical examination [64], but further research is needed to substantiate this finding, especially with respect to the temporal effects of the two pathological processes on overall signal change.

Interpretation of muscle signal change must be taken in context with various factors, related to degree of nerve injury, anatomical variation and co-existent muscle pathology. Partial denervation or collateral innervation may result in delayed or absent signal changes [78]. Inflammatory myopathies, rhabdomyolysis, compartment syndrome or tumour involvement of muscle can cause identical T2-weighted signal changes [79] but not in classic myotomal distributions of certain CEN syndromes. Fatty replacement in muscle may occur in Duchenne's muscular dystrophy, poliomyelitis, collagen disorders and cerebrovascular accidents, which may be diffuse or stranded in appearance [80].

## Conclusion

The fundamental diagnosis of CEN remains clinical and electrophysiological studies backed up by surgical exploration where indicated; however, radiologists are increasingly evaluating CEN in equivocal or atypical cases. Although many papers have described new techniques and their accuracy compared with the above current gold standards, there is little evidence to suggest significant impact of imaging on patient outcome in the commoner syndromes.

Evidence comparing diagnostic accuracy of MRI vs US is also lacking, and ultimately the choice of imaging

modality lies with the personal preferences of the radiologist. The contribution of diagnostic radiology in patient management is most compelling for exclusion of mass lesions, especially where therapeutic-guided intervention may be an option. Preoperative planning with precise localisation of lesions, may avoid the need for exploratory surgery, allowing for smaller targeted exposures. Surgical technique and the need for intraoperative electrophysiological monitoring may depend on the distinction between perineural and intraneural masses.

A targeted approach based on the clinical findings, utilising the latest technology is the mainstay of radiological CEN diagnosis, especially where underlying predisposing conditions for CEN exist; however, there remain many controversial issues regarding the predictive value of many imaging features of CEN, particularly with regard to the median nerve in CTS.

Further advances in MR and US technology may revolutionise the contribution of imaging in the evaluation of CEN, but well performed studies will be required to adequately assess the impact of emerging technology. In the meantime, important clues do exist for the eagle-eyed radiologist on plain films!

## References


1. Bosch EP, Smith BE (2000) Disorders of peripheral nerves. In: Bradley G, Daroff R, Fenichel G, Marsden CD (eds) Neurology in clinical practice, the neurological disorders. Butterworth-Heinemann, Boston, p 2056
2. Brumback RA, Bobele GB, Rayan GM (1992) Electrodiagnosis of compressive nerve lesions. Hand Clin 8:241–254
3. Kaufman MA (1996) Differential diagnosis and pitfalls in electrodiagnostic studies and special tests for diagnosing compressive neuropathies. Orthop Clin North Am 27:245–252
4. Radecki P (1995) Variability in the median and ulnar nerve latencies: implications for diagnosing entrapment. J Occup Environ Med 37:1293–1299
5. Chen WS (1995) Median-nerve neuropathy associated with chronic anterior dislocation of the lunate. J Bone Joint Surg Am 77:1853–1857
6. Bianchi S, Martinoli C, Abdelwahab IF (1999) High-frequency ultrasound examination of the wrist and hand. Skeletal Radiol 28:121–129
7. Masciocchi C, Catalucci A, Barile A (1998) Ankle impingement syndromes. Eur J Radiol 27 (Suppl 1):S70–S73
8. Lanteri M, Ptasznik R, Constable L, Dawborn JK (1997) Ultrasound changes in the wrist and hand in hemodialysis patients. Clin Nephrol 48:375–380
9. Chen CK, Chung CB, Yeh L, Pan HB, Yang CF, Lai PH, Liang HL, Resnick D (2000) Carpal tunnel syndrome caused by tophaceous gout: CT and MR imaging features in 20 patients. AJR 175:655–659
10. Sallomi D, Janzen DL, Munk PL, Connell DG, Tirman PF (1998) Muscle denervation patterns in upper limb nerve injuries: MR imaging findings and anatomic basis. AJR 171:779–784
11. Mondelli M, Cioni R, Federico A (1998) Rare mononeuropathies of the upper limb in bodybuilders. Muscle Nerve 21:809–812
12. Bianchi S, Abdelwahab IF, Zwass A, Giacomello P (1994) Ultrasonographic evaluation of wrist ganglia. Skeletal Radiol 23:201–203
13. Hashimoto BE, Hayes AS, Ager JD (1994) Sonographic diagnosis and treatment of ganglion cysts causing suprascapular nerve entrapment. J Ultrasound Med 13:671–674
14. Laurencin CT, Schwartz JT, Koris MJ (1994) Compression of the ulnar nerve at the elbow in association with synovial cysts. Orthop Rev 23:62–65
15. Gibbon AJ, Wardell SR, Scott RD (1999) Synovial cyst of the proximal tibiofibular joint with peroneal nerve compression after total knee arthroplasty. J Arthroplasty 14:766–768
16. Bianchi S, Abdelwahab IF, Zwass A, Calogera R, Banderali A, Brovero P, Votano P (1993) Sonographic findings in examination of digital ganglia: retrospective study. Clin Radiol 48:45–47
17. O'Driscoll SW, Horii E, Carmichael SW, Morrey BF (1991) The cubital tunnel and ulnar neuropathy. J Bone Joint Surg Br 73:613–617
18. Anderson MW, Benedetti P, Walter J, Steinberg DR (1995) MR appearance of the extensor digitorum manus brevis muscle: a pseudotumor of the hand. AJR 164:1477–1479
19. Paik NJ, Han TR, Lim SJ (2000) Multiple peripheral nerve compressions related to malignantly transformed hereditary multiple exostoses. Muscle Nerve 23:1290–1294
20. Wittenberg KH, Adkins MC (2000) MR imaging of nontraumatic brachial plexopathies: frequency and spectrum of findings. Radiographics 20:1023–1032
21. Van Es HW (2001) MRI of the brachial plexus. Eur Radiol 11:325–336
22. Kim YS, Yeh LR, Trudell D, Resnick D (1998) MR imaging of the major nerves about the elbow: cadaveric study examining the effect of flexion and extension of the elbow and pronation and supination of the forearm. Skeletal Radiol 27:419–426
23. Panegyres PK, Moore N, Gibson R, Rushworth G, Donaghy M (1993) Thoracic outlet syndromes and magnetic resonance imaging. Brain 116:823–841
24. Smedby O, Rostad H, Klaastad O, Lilleas F, Tillung T, Fosse E (2000) Functional imaging of the thoracic outlet syndrome in an open MR scanner. Eur Radiol 10:597–600
25. Spinner RJ, Lins RE, Collins AJ, Spinner M (1993) Posterior interosseous nerve compression due to an enlarged bicipital bursa confirmed by MRI. J Hand Surg [Br] 18:753–756
26. Yanagisawa H, Okada K, Sashi R (2001) Posterior interosseous nerve palsy caused by synovial chondromatosis of the elbow joint. Clin Radiol 56:510–514
27. Inokuchi W, Ogawa K, Horiuchi Y (1998) Magnetic resonance imaging of suprascapular nerve palsy. J Shoulder Elbow Surg 7:223–227
28. Martinoli C, Serafini G, Bianchi S, Bertolotto M, Gandolfo N, Derchi LE (1996) Ultrasonography of peripheral nerves. J Peripher Nerv Syst 1:169–178
29. Martinoli C, Derchi LE, Bertolotto M, Gandolfo N, Bianchi S, Fiallo P, Nunzi E (2000) US and MR imaging of peripheral nerves in leprosy. Skeletal Radiol 29:142–150
30. Okamoto M, Abe M, Shirai H, Ueda N (2000) Morphology and dynamics of the ulnar nerve in the cubital tunnel. Observation by ultrasonography. J Hand Surg [Br] 25:85–89

31. Buchberger W, Judmaier W, Birbamer G, Lener M, Schmidauer C (1992) Carpal tunnel syndrome: diagnosis with high-resolution sonography. AJR 159:793–798
32. Chen P, Maklad N, Redwine M, Zelitt D (1997) Dynamic high-resolution sonography of the carpal tunnel. AJR 168:533–537
33. Oh SJ, Meyer RD (1999) Entrapment neuropathies of the tibial (posterior tibial) nerve. Neurol Clin 17:593–615
34. Fornage BD (1988) Peripheral nerves of the extremities: imaging with US. Radiology 167:179–182
35. Hide IG, Grainger AJ, Naisby GP, Campbell RS (1999) Sonographic findings in the anterior interosseous nerve syndrome. J Clin Ultrasound 27:459–464
36. Silvestri E, Martinoli C, Derchi LE, Bertolotto M, Chiaramondia M, Rosenberg I (1995) Echotexture of peripheral nerves: correlation between US and histologic findings and criteria to differentiate tendons. Radiology 197:291–296
37. Filler AG, Kliot M, Howe FA, Hayes CE, Saunders DE, Goodkin R, Bell BA, Winn HR, Griffiths JR, Tsuruda JS (1996) Application of magnetic resonance neurography in the evaluation of patients with peripheral nerve pathology. J Neurosurg 85:299–309
38. Britz G, West G, Dailey A (1995) Magnetic resonance imaging in evaluating and treating peripheral nerve problems. Perspect Neurol Surg 6:53–66
39. Aagaard BD, Maravilla KR, Kliot M (1998) MR neurography. MR imaging of peripheral nerves. Magn Reson Imaging Clin North Am 6:179–194
40. Patel VV, Heidenreich FP, Bindra RR, Yamaguchi K, Gelberman RH (1998) Morphologic changes in the ulnar nerve at the elbow with flexion and extension: a magnetic resonance imaging study with 3-dimensional reconstruction. J Shoulder Elbow Surg 7:368–374
41. Kuntz C, Blake L, Britz G, Filler A, Hayes CE, Goodkin R, Tsuruda J, Maravilla K, Kliot M (1996) Magnetic resonance neurography of peripheral nerve lesions in the lower extremity. Neurosurgery 39:750–757
42. Sugimoto H, Miyaji N, Ohsawa T (1994) Carpal tunnel syndrome: evaluation of median nerve circulation with dynamic contrast-enhanced MR imaging. Radiology 190:459–466
43. Nakamichi K, Tachibana S (1995) Restricted motion of the median nerve in carpal tunnel syndrome. J Hand Surg [Br] 20:460–464
44. Keberle M, Jenett M, Kenn W, Reiners K, Peter M, Haerten R, Hahn D (2000) Technical advances in ultrasound and MR imaging of carpal tunnel syndrome. Eur Radiol 10:1043–1050
45. Duncan I, Sullivan P, Lomas F (1999) Sonography in the diagnosis of carpal tunnel syndrome. AJR 173:681–684
46. Redd RA, Peters VJ, Emery SF, Branch HM, Rifkin MD (1989) Morton neuroma: sonographic evaluation. Radiology 171:415–417
47. Shapiro PP, Shapiro SL (1995) Sonographic evaluation of interdigital neuromas. Foot Ankle Int 16:604–606
48. Sobiesk GA, Wertheimer SJ, Schulz R, Dalfovo M (1997) Sonographic evaluation of interdigital neuromas. J Foot Ankle Surg 36:364–366
49. Gebarski SS, Telian SA, Niparko JK (1992) Enhancement along the normal facial nerve in the facial canal: MR imaging and anatomic correlation. Radiology 183:391–394
50. Dawson DM (1993) Entrapment neuropathies of the upper extremities. N Engl J Med 329:2013–2018
51. Healy C, Watson JD, Longstaff A, Campbell MJ (1990) Magnetic resonance imaging of the carpal tunnel. J Hand Surg [Br] 15:243–248
52. Munk PL, Vellet AD, Levin MF, Steinbach LS, Helms CA (1992) Current status of magnetic resonance imaging of the wrist. Can Assoc Radiol J 43:8–18
53. Murphy RX, Chernofsky MA, Osborne MA, Wolson AH (1993) Magnetic resonance imaging in the evaluation of persistent carpal tunnel syndrome. J Hand Surg [Am] 18:113–120
54. Rosenbaum RB (1993) The role of imaging in the diagnosis of carpal tunnel syndrome. Invest Radiol 28:1059–1062
55. Weiss KL, Beltran J, Lubbers LM (1986) High-field MR surface-coil imaging of the hand and wrist. Part II. Pathologic correlations and clinical relevance. Radiology 160:147–152
56. Radack DM, Schweitzer ME, Taras J (1997) Carpal tunnel syndrome: Are the MR findings a result of population selection bias? AJR 169:1649–1653
57. Mesgarzadeh M, Triolo J, Schneck CD (1995) Carpal tunnel syndrome. MR imaging diagnosis. Magn Reson Imaging Clin North Am 3:249–264
58. Koenig H, Lucas D, Meissner R (1986) The wrist: a preliminary report on high-resolution MR imaging. Radiology 160:463–467
59. Middleton WD, Kneeland JB, Kellman GM, Cates JD, Sanger JR, Jesmanowicz A, Froncisz W, Hyde JS (1987) MR imaging of the carpal tunnel: normal anatomy and preliminary findings in the carpal tunnel syndrome. AJR 148:307–316
60. Brahme SK, Resnick D (1991) Magnetic resonance imaging of the wrist. Rheum Dis Clin North Am 17:721–739
61. Monagle K, Dai G, Chu A, Burnham RS, Snyder RE (1999) Quantitative MR imaging of carpal tunnel syndrome. AJR 172:1581–1586
62. Allmann KH, Horch R, Uhl M, Gufler H, Altehoefer C, Stark GB, Langer M (1997) MR imaging of the carpal tunnel. Eur J Radiol 25:141–145
63. Horch RE, Allmann KH, Laubenberger J, Langer M, Stark GB (1997) Median nerve compression can be detected by magnetic resonance imaging of the carpal tunnel. Neurosurgery 41: 76–82
64. Britz GW, Haynor DR, Kuntz C, Goodkin R, Gitter A, Kliot M (1995) Carpal tunnel syndrome: correlation of magnetic resonance imaging, clinical, electrodiagnostic, and intraoperative findings. Neurosurgery 37:1097–1103
65. Seyfert S, Boegner F, Hamm B, Kleindienst A, Klatt C (1994) The value of magnetic resonance imaging in carpal tunnel syndrome. J Neurol 242:41–46
66. Rosenberg ZS, Bencardino J, Beltran J (1997) MR features of nerve disorders at the elbow. Magn Reson Imaging Clin North Am 5:545–565
67. Hayes CE, Tsuruda JS, Mathis CM, Maravilla KR, Kliot M, Filler AG (1997) Brachial plexus: MR imaging with a dedicated phased array of surface coils. Radiology 203:286–289
68. Spratt JD, Logan BM, Abrahams PH (1996) Variant slips of psoas and iliacus muscles, with splitting of the femoral nerve. Clin Anat 9:401–404
69. Howe FA, Filler AG, Bell BA, Griffiths JR (1992) Magnetic resonance neurography. Magn Reson Med 28:328–338
70. Filler AG, Golden RN, Howe FA (1993) High resolution diffusion gradient imaging for neurography in human subjects (abstract). In: Proc Soc Magnetic Resonance in Medicine. Society of Magnetic Resonance in Medicine, Berkley, Calif. p 101
71. Filler AG (1994) Axonal transport and MR imaging: prospects for contrast agent development. J Magn Reson Imaging 4:259–267
72. Bonel HM, Heuck A, Frei KA, Herrmann K, Scheidler J, Srivastav S, Reiser M (2001) Carpal tunnel syndrome: assessment by turbo spin echo, spin echo, and magnetization transfer imaging applied in a low-field MR system. J Comput Assist Tomogr 25:137–145

73. Entrekin RR, Porter BA, Sillesen HH, Wong AD, Cooperberg PL, Fix CH (2001) Real-time spatial compound imaging: application to breast, vascular, and musculoskeletal ultrasound. Semin Ultrasound CT MR 22:50–64
74. Gunreben G, Bogdahn U (1991) Real-time sonography of acute and chronic muscle denervation. Muscle Nerve 14:654–664
75. Bredella MA, Tirman PF, Fritz RC, Wischer TK, Stork A, Genant HK (1999) Denervation syndromes of the shoulder girdle: MR imaging with electrophysiologic correlation. Skeletal Radiol 28:567–572
76. Linker CS, Helms CA, Fritz RC (1993) Quadrilateral space syndrome: findings at MR imaging. Radiology 188:675–676
77. Grainger AJ, Campbell RS, Stothard J (1998) Anterior interosseous nerve syndrome: appearance at MR imaging in three cases. Radiology 208:381–384
78. Fleckenstein JL, Watumull D, Conner KE, Ezaki M, Greenlee RG Jr, Bryan WW, Chason DP, Parkey RW, Peshock RM, Purdy PD (1993) Denervated human skeletal muscle: MR imaging evaluation. Radiology 187:213–218
79. Uetani M, Hayashi K, Matsunaga N, Imamura K, Ito N (1993) Denervated skeletal muscle: MR imaging. Work in progress. Radiology 189:511–515
80. Sebag G, Dubois J (1994) The soft tissues. In: Carty H, Brunette F, Shaw D, Kendall B (eds) Imaging children. Churchill Livingstone, New York, pp 1366–1367